2012

Weakly anomalous diffusion with non-Gaussian propagators

PHYSICAL REVIEW E, COLLEGE PK, v. 86, n. 2, pp. 157-160, AUG 27, 2012
http://www.producao.usp.br/handle/BDPI/33797

Weakly anomalous diffusion with non-Gaussian propagators

J. C. Cressoni,[1,2] G. M. Viswanathan,[2,3] A. S. Ferreira,[4] and M. A. A. da Silva[1]
[1]*Departamento de Física e Química, FCFRP, Universidade de São Paulo, Ribeirão Preto, SP 14040-903, Brazil*
[2]*Instituto de Física, Universidade Federal de Alagoas, Maceió, AL 57072-970, Brazil*
[3]*Departamento de Física Teórica e Experimental, Universidade Federal do Rio Grande do Norte, Natal, RN 59078-900, Brazil*
[4]*Departamento de Física, Universidade Federal de Pernambuco, Recife, PE 50670-901, Brazil*
(Received 6 January 2012; published 27 August 2012)

A poorly understood phenomenon seen in complex systems is diffusion characterized by Hurst exponent $H \approx 1/2$ but with non-Gaussian statistics. Motivated by such empirical findings, we report an exact analytical solution for a non-Markovian random walk model that gives rise to weakly anomalous diffusion with $H = 1/2$ but with a non-Gaussian propagator.

DOI: 10.1103/PhysRevE.86.022103 PACS number(s): 05.40.−a, 89.75.−k, 02.50.−r, 89.65.Gh

Introduction. Anomalous diffusion [1–4] generalizes the study of normal diffusion, which began with the pioneering contributions of Fourier, Brown, Fick, Bachelier, and Einstein. In normal diffusion the mean square displacement grows linearly with time. Moreover, the random walk propagators which give the probability density of finding a particle at position x_2 at time t_2 starting from position x_1 at time t_1 converge to a Gaussian for large times $|t_2 - t_1| \to \infty$. In anomalous diffusion, mean square displacements usually grow either sublinearly or superlinearly but not linearly, i.e., $\langle x^2 \rangle \sim t^{2H}$, with $H \neq 1/2$. In the results that follow, the mean position $\langle x \rangle$ is not stationary, so we follow the convention by studying the scaling of $\langle (x - \langle x \rangle)^2 \rangle$ instead of $\langle x^2 \rangle$. The exponent H is known as the Hurst exponent and is one of the most important quantities in the study of anomalous diffusion. Subdiffusion ($H < 1/2$) and superdiffusion ($H > 1/2$) have been studied in diverse systems, and their theoretical basis is now well understood [3]. However, there is a marginal case which is of great importance but which remains very poorly understood: Diffusion with $H = 1/2$ but with non-Gaussian propagators. Our goal is to understand better this phenomenon, which we refer to henceforth as weakly anomalous diffusion. This phenomenon has only been observed experimentally, but the underlying physics has never been properly understood. Here we present a model that contains the essential ingredients to reproduce weakly anomalous diffusion. As a bonus, we obtain the exact analytical solution.

Weakly anomalous diffusion is seen in real complex systems, yet diffusion with $H \approx 1/2$ but with non-Gaussian propagators is nevertheless counterintuitive. The central limit theorem which applies to normal diffusion with $H = 1/2$ also guarantees Gaussian propagators given the usual conditions. Specifically, Gaussian propagators are guaranteed (at long times) for Markovian random walks whose step size distributions have finite variance. Even non-Markovian processes, such as fractional Brownian motions (e.g., single file diffusion [5,6]), are described by Gaussian propagators. However, there are classic empirical findings of diffusive phenomena with $H = 1/2$ for which the propagators are nevertheless non-Gaussian. A remarkable example of weakly anomalous diffusion is the fluctuation of returns in financial markets. The log-returns, the logarithm of the returns, have vanishing two-point autocorrelation at long times, consistent with $H = 1/2$. But hidden underneath the apparently uncorrelated returns are long-range power law correlations in the absolute value of the log-returns: memory effects which render the process non-Markovian. The empirically measured propagator is strongly non-Gaussian, even though $H \approx 1/2$ [7].

This gap in our present understanding motivates the study of random walk models which can reproduce weakly anomalous diffusion. There is a long tradition in statistical physics of using limiting models that capture the essential ingredients of physical systems to study real phenomena. Examples include the use of the self-avoiding walk to model real polymer chains and the simple Ising model for studying real magnetic systems. We adopt this strategy and ask what is the simplest possible non-Markovian random walk which gives rise to weakly anomalous diffusion. The results we report below show clearly how long-range memory effects can change H and the propagator independently. Our results also have a bearing on the family of autoregressive and heteroscedastic processes, some of which have a bearing on anomalous diffusion [8–21].

Model. The model we propose describes the motion of a random walker in one dimension, which was inspired by the so-called elephant [22] and Alzheimer [23] walks. In the latter models, the walker remembers either the complete history (elephant) or an initial fraction of the history (Alzheimer). In contrast, in our model the walker remembers only a single but moving point in time.

In each time step, the walker currently at position X_t moves one step to the right or left to X_{t+1}, according to a probabilistic recurrence relation:

$$X_{t+1} = X_t + \sigma_{t+1}, \tag{1}$$

where X_{t+1} is the new position and $\sigma_{t+1} = \pm 1$ represents a stochastic noise that contains two-point correlations (i.e., memory). From the entire history of prior random walk step directions $\{\sigma_{t'}\}$, only the decision taken at the previous time $t' = ft$ is used at time t, with fixed $0 < f < 1$. The current step direction σ_t is based on the value of $\sigma_{t'}$ at time $t' = ft$ in the following manner:

$$\sigma_t = \begin{cases} +\sigma_{t'} & \text{with probability} \quad p, \\ -\sigma_{t'} & \text{with probability} \quad 1 - p. \end{cases} \tag{2}$$

Without loss of generality we assume that the first step always goes to the right, i.e., $\sigma_1 = +1$, and t' must be an integer value,

as time is discrete. Therefore one must actually set $t' = \lfloor ft \rfloor$, i.e., the largest integer smaller than ft. The position at time t thus follows $X_t = \sum_{t'=1}^{t} \sigma_{t'}$, and for the sake of simplicity we assume that $X_0 = 0$ for $t = 0$.

Results. We now solve the model. An equation for the first moment can be obtained by considering effective probabilities $P^+(t)$ and $P^-(t)$ of moving to the right or left, respectively, so that $P^-(t') + P^+(t') = 1$. Define $P^+(t)$ as

$$\begin{aligned} P^+(t) &= pP^+(t') + (1-p)[1 - P^+(t')] \\ &= \alpha P^+(t') + \frac{1-\alpha}{2}, \end{aligned} \tag{3}$$

with $\alpha = 2p - 1$. Since $t' = ft$, we can write

$$P^+(t') = \alpha P^+(f^2 t) + \frac{1-\alpha}{2}, \tag{4}$$

which leads to a recursive relation,

$$P^+(t) = \alpha^n P^+(f^n t) + \left(\frac{1-\alpha^n}{2}\right). \tag{5}$$

In the asymptotic limit we can write the speed of the random walker as $d\langle x\rangle/dt = \sigma^{\text{eff}} = P^+ - P^-$ or

$$\begin{aligned} \frac{d\langle x\rangle}{dt} &= 2\left[\alpha^n P^+(f^n t) + \left(\frac{1-\alpha^n}{2}\right)\right] - 1 \\ &= \alpha^n [2P^+(f^n t) - 1], \end{aligned} \tag{6}$$

where $\langle x\rangle$ stands for the first moment and ensemble average is assumed. The last stage of the iteration is $t' = f^N t = 0$, which will be reached for some integer $N = N(t)$. Prior to this last iteration step we can write $f^{N-1}t = A$, where A is some positive integer. Therefore, for $n = N$ we can write $P^+(f^N t) = P^+(0) = 1$, where $P^+(0) = 1$ represents the initial condition. Then, Eq. (6) becomes

$$\frac{d\langle x\rangle}{dt} = \alpha^N, \tag{7}$$

with $N = N(t)$, which is the basic equation to be solved in order to fully describe this model. We then seek to solve (7) for $v = d\langle x\rangle/dt$, with N given by $f^{N-1}t = A$, or $N = \ln t/\ln f^{-1} - \ln A/\ln f^{-1} + 1$, where $A \geqslant 1$ is some integer that depends on f and t.

The solution of (7) is straightforward for $\alpha = 0$ or $p = 1/2$. In this case $d\langle x\rangle/dt = 0$, so $\langle x\rangle$ does not depend on t. Due to the initial condition $\langle x(0)\rangle = 0$, we get $\langle x(t)\rangle = 0$. This is memoryless Brownian motion ($p = 1/2$ in this model).

We now consider the case $\alpha > 0$. Equation (7) can be written as

$$\frac{d\langle x\rangle}{dt} = B\alpha^{\ln t/(\ln f^{-1})} = Bt^{\ln\alpha/(\ln f^{-1})}, \tag{8}$$

with $B = |\alpha|^{-(\ln A)/(\ln f^{-1})+1}$. Here we must distinguish two cases: one that leads to a power law for $\langle x(t)\rangle$ and one that leads to a logarithmic solution. The latter happens for $\ln\alpha/\ln f^{-1} = -1$ (i.e., $\alpha = f$ or $2p - 1 = f$) for which the equation becomes $d\langle x\rangle/dt = B/t$, which gives

$$\langle x(t)\rangle = B\ln t + C. \tag{9}$$

For $\ln\alpha/\ln f^{-1} \neq -1$ we can perform a direct integration, i.e.,

$$\langle x(t)\rangle = B\frac{t^{(\ln\alpha)/(\ln f^{-1})+1}}{(\ln\alpha)/(\ln f^{-1}) + 1} = B\frac{t^\delta}{\delta}, \tag{10}$$

where we set the integration constant to zero due to the initial condition $\langle x(0)\rangle = 0$ and defined the parameter

$$\delta = (\ln\alpha)/(\ln f^{-1}) + 1, \tag{11}$$

which will be extensively used throughout the rest of this Brief Report. We need to be more careful when $\alpha < 0$ because α^N oscillates between positive and negative values as N is even or odd. A direct integration becomes difficult because the function has a great number of discontinuities. For $\alpha < 0$ we can write Eq. (7) as

$$\frac{d\langle x\rangle}{dt} = (-|\alpha|)^N = (-1)^N|\alpha|^N. \tag{12}$$

A full solution for Eq. (12) can be obtained by writing a Fourier series expansion for the square wave $(-1)^N$, which gives

$$\frac{d\langle x\rangle}{ds} = -\frac{4B}{\pi}\sum_{m=0}^{\infty}\frac{1}{2m+1}\sin\left(\frac{2m+1}{\lambda}\pi s\right)e^{(1+\ln|\alpha|/\lambda)s}, \tag{13}$$

with $\lambda = \ln f^{-1}$ and $s = \ln t$. This equation can be integrated directly in s to give

$$\begin{aligned} \langle x(t)\rangle &= -\frac{4B}{\pi}t^\delta\sum_{m=0}^{\infty}\left(\frac{1}{2m+1}\right)\frac{\sin[a_m(\ln t + s_0) - \phi_m]}{\sqrt{a_m^2 + \delta^2}} + C \\ &= t^\delta S(\ln t) + C, \end{aligned}$$

where C is an integration constant, $a_m = [(2m+1)/(\ln f^{-1})]\pi$, $\phi_m = \arccos[\delta/(a_m^2 + \delta^2)^{1/2}]$, and s_0 is a shift to adjust the solution to the initial condition. The sum and other factors have been collected inside the function $S(\ln t)$, defined for convenience.

We now turn our attention to the second moment $\langle x^2(t)\rangle \equiv \langle X_t^2\rangle$, whose asymptotic behavior is important to determine the Hurst exponent. Starting with the basic equation of motion (1), we can write $\langle X_{t+1}^2\rangle - \langle X_t^2\rangle = 2\langle\sigma_{t+1}X_t\rangle + 1$. Therefore we can define the second moment derivative,

$$\frac{d\langle x^2\rangle}{dt} = 1 + 2\langle\sigma_{t+1}X_t\rangle, \tag{14}$$

where the explicit time dependence of $\langle x^2(t)\rangle$ was dropped.

The exact evaluation of the second moment is more challenging because of the correlation function appearing on the right hand side. We have used several approaches to reach an exact solution, but the results are still incomplete. Fortunately, however, we can carry on the discussion about the nature of the diffusive regimes based solely on the exact information available for the asymptotic behavior of the first moment. In what follows, we show how to derive exact expressions for the Hurst exponent, allowing a complete characterization of the phase diagram and analytical determination of the critical separation lines.

We have argued before [24] that the diffusion behavior is normal if the scaling exponent of $\langle x(t)\rangle$ is $\delta \leqslant 1/2$. The Hurst

exponent is then given by $H = 1/2$. For the convenience of the reader we hereby reproduce the main arguments that give support to this result. Based on experimental observations, we have conjectured that $H = \delta$ is valid throughout the superdiffusive regime, provided that there is no subdiffusion (the model we discuss does not present subdiffusion since other ingredients would then be necessary, e.g., traps in the system [25]). Although a general proof is still lacking, the conjecture has been rigorously proved for a quite general model presenting amnestically induced persistence [24] and is supported by the following reasoning: a ballistic motion leads trivially to $H = \delta$; it is therefore reasonable to assume that $H = \delta = 1 - \epsilon$ (ϵ very small) for a motion near the ballistic regime. By inductive reasoning we can conclude that this must be true up to the transition line, where $H = \delta = 1/2$. Since there is no subdiffusion, the regime must be normal with $H = 1/2$ within the region corresponding to $\delta \leqslant 1/2$. In conclusion, we have $H = 1/2$ for $\delta \leqslant 1/2$ and $H = \delta$ for $\delta > 1/2$. This has been confirmed by computing simulations for $\langle x^2 \rangle$. The case $\delta > 1/2$, however, remains elusive. In this case, since $H = \delta$, $\langle x^2 \rangle \sim t^{2H}$, and $\langle x \rangle \sim t^{\delta}$ [from Eq. (10)], we can write $\langle x^2 \rangle \sim \langle x \rangle^2$ (i.e., they have the same scaling behavior). The regime is therefore either superdiffusive with $H = \delta > 1/2$ or normally diffusive ($H = 1/2$) with escape. In the latter case $\langle x^2 \rangle = \langle x \rangle^2$ plus correction terms, which was not observed in the simulations. The experiments indeed show the same scaling behavior for the variance and the second moment, thereby indicating superdiffusive behavior. Rigorously, however, we prefer to leave the true diffusive nature of the walk as inconclusive since the asymptotic limit may not yet have been reached. We are currently looking for an exact solution for this problem.

We therefore settle for two normal diffusive regimes, one for $\delta < 0$ and another for $0 < \delta < 1/2$. Although the Hurst exponent is $H = 1/2$ in both cases, the behavior of the walk is not the same, as can be seen from the asymptotic behavior of $\langle x \rangle$. For $\delta < 0$ the random walk performs a localized walk, never going too far from the origin. This regime represents well a normal diffusion. On the other hand, for $0 < \delta < 1/2$ the first moment diverges in the asymptotic limit. This case is a normal diffusion regime with escape. But is it really normal diffusion? The computing simulations show that although $H = 1/2$, the regime for $0 < \delta < 1/2$ is characterized by non-Gaussian propagators. This important point of this Brief Report is discussed below.

Notice that although we cannot give a definite answer as to the nature of the diffusion for $\delta > 1/2$, we can safely say that it represents a fast escape walk, in contrast to the walk with $0 < \delta < 1/2$. Therefore the corresponding region in the phase diagram is either a superdiffusive region or a normally diffusive region with fast escape. This question calls for more detailed studies, which are currently being addressed.

Figure 1 shows the complete phase diagram on the (f, p) plane. The parabola for $\delta = 1/2$ (or $f = 4p^2 - 4p + 1$) sets a discontinuity in the asymptotic behavior of $\langle x^2 \rangle$. For $\delta > 1/2$ ($0 < \delta < 1/2$) we have a fast (slow) escape regime for all α. For $\alpha < 0$ ($p < 1/2$), the escape regime disappears on the $\delta = 0$ line, but the log-periodicity remains. For $\alpha > 0$ ($p > 1/2$), the solution for $\langle x \rangle$ is given by (10). Again, $\delta = 0$ divides the $p > 1/2$ region in two: one below (escape regime, $\delta > 0$) for which $x(t) \to \infty$ and one above (normally diffusive, $\delta < 0$) for which $x(t) \to 0$, asymptotically. On the $\delta = 0$ line itself, the solution is logarithmic, as given by (9). It is still an escape regime since $x(t)$ diverges, unlike what was found for $p < 1/2$. It is, however, slowly divergent. Experimentally, we have found that this logarithmic regime manifests itself after an initial transient (not shown).

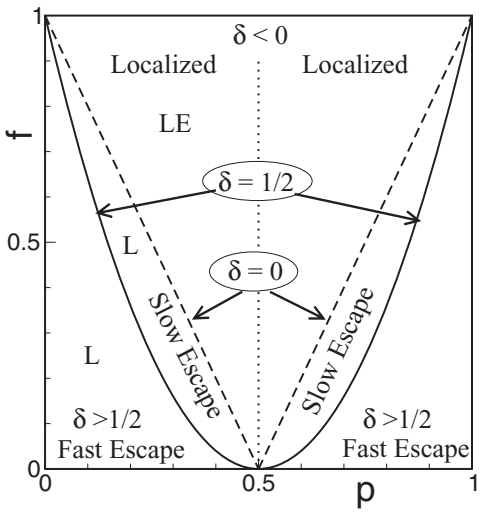

FIG. 1. The richness of the f-p phase diagram. The parabola ($\delta = 1/2$) separates the two escape regimes. The dashed lines ($\delta = 0$) separate the localized and slow escape regimes. The vertical dotted line ($p = 1/2$) separates the log-periodic (L) region on the left and the non-log-periodic region on the right.

Figure 2 shows selected log-periodic solutions for $\langle x(t) \rangle$, all for $p < 1/2$. Typical solutions for the fast escape regime are shown in Figure 2(a), both analytically and numerically. The sharp peaks are a direct consequence of the memory

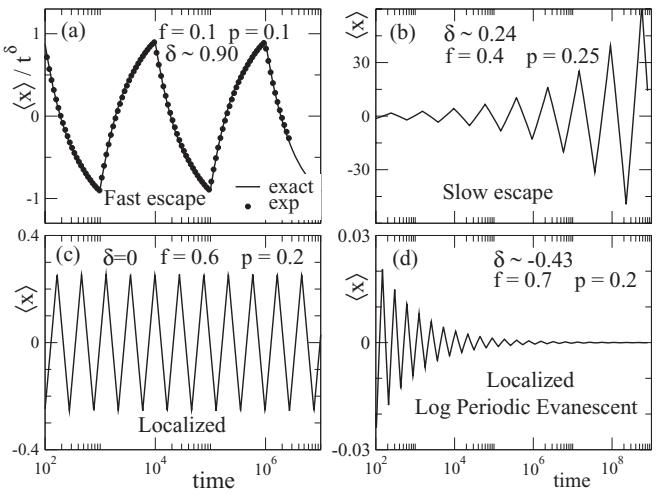

FIG. 2. Examples of solutions for $\langle x(t) \rangle$ within the log-periodic region ($p < 1/2$). (a) Exact and experimental solutions, normalized for visual aid. The experimental observations were obtained with 10^3 runs with 6×10^6 total time units each. (b) The escape regime associated with $0 < \delta < 1/2$. (c) and (d) The localized regimes. The log-periodic solution for $\delta < 0$ in (d) fades away in the asymptotic limit.

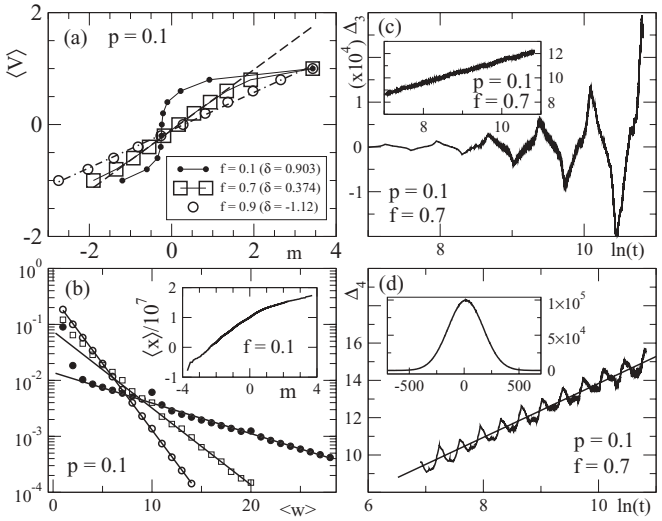

FIG. 3. (a) Gaussian probability plot of the speed of the random walker measured after 10^8 time units, calculated using $v = [x(10^8 + 10) - x(10^8)]/10$ vs the normal order statistic medians m. Three cases are shown: $f = 0.1$ (solid circles, $\delta \approx 0.90$), $f = 0.7$ (squares, $\delta \approx 0.37$), and $f = 0.9$ (open circles, $\delta \approx -1.12$), all for $p = 0.1$. They correspond, respectively, to the fast escape, slow escape, and normal localized regimes. The straight line for $\delta < 0$ indicates Gaussian behavior. (b) The persistence length distributions corresponding to the same parameters (f, p) as above. The inset shows the corresponding Gaussian probability plot for position $\langle x \rangle$ ($f = 0.1$) vs the normal order statistics medians m. The propagator is visibly non-Gaussian. (c) The difference $\Delta_3 = 3\langle x \rangle [\langle x^2 \rangle - \langle x \rangle^2] - [\langle x^3 \rangle - \langle x \rangle^3]$ as a function of $\ln t$. This difference is equal to zero for a Gaussian distribution. The inset shows Δ_3 for $\alpha > 0$. (d) The difference $\Delta_4 = 3[\langle x^2 \rangle^2 - \langle x \rangle^4] - [\langle x^4 \rangle - \langle x \rangle^4]$ as a function of t in a log-log plot. This also is identically equal to zero for Gaussian distributions. The straight line represents a linear fit. The inset shows the form of the distribution of the position, but any resemblance to a Gaussian distribution is misleading (see text).

profile consisting of δ distributions at ft, with the Fourier expansion for the square wave $(-1)^N$ leading naturally to this type of solution. As expected from (14), we can clearly see the log-periodic solutions for $\delta > 0$ and $p < 1/2$. For $\delta > 0$ the random walk escapes to infinity with a scaling exponent equal to $1/2$. The $\delta < 0$ regime can be termed "log-periodic evanescent" because, although the random walker position oscillates, the walker stays localized around the origin since $x(t) \to 0$ as t gets larger and larger.

Discussion and conclusion. Now we can see why we should expect non-Gaussian propagators. Even though $H = 1/2$, the first moment can be highly nonstationary and can oscillate log-periodically, so that the propagator cannot easily retain its shape. The tails of the propagator cannot rearrange themselves and move in synchrony with the peak or central part of the propagator. The log-periodic oscillations prevent convergence towards a stable (Gaussian) shape. Figure 3 shows this surprising effect whereby normal diffusion can be associated with non-Gaussian propagators. Figure 3(a) shows the speed of the random walker versus the normal order statistic medians m as usual, after 10^8 time units with 10^4 runs. A straight line implies a Gaussian probability distribution. Notice that the localized regime ($\delta < 0$) is well fitted by a straight line (dot-dashed line) indicating a Gaussian propagator, as expected. However, both escape regimes ($\delta > 0$) show remarkable deviations from Gaussian behavior (the dashed line is a linear fit and the continuous thin lines are just connecting lines). Figure 3(b) shows the persistence length distributions on a log-linear plot, corresponding to the same parameters (f, p) shown in Fig. 3(a). Gaussian propagators present exponential persistence length distributions. The departure from the exponential behavior is appreciable, and we see nonexponential behavior for $f = 0.7$ and $f = 0.1$, inconsistent with Gaussian propagators. The inset is a probability plot ($f = 0.1$) drawn with the logarithm of the distribution data, also confirming nonexponential behavior. The normal probability plots were drawn by plotting the ordered sample data against the order statistic medians. The latter are related to the inverse of the standard normal cumulative distribution function. If the plot is linear, then the data are normally distributed [26]. The length of persistence was counted after $T_{\min} = 10^6$, and the data were statistically averaged over 10^3 runs (convergence tested for 8×10^3 runs). The spikes (and their period) showing up for $f = 0.7$ and $f = 0.1$ can be shown to be a consequence of the sharp peaks (and their periods) in the analytic solution shown in Fig. 2(a). The straight lines were fitted to the tail of the distribution excluding the spikes ($f = 0.7$ and $f = 0.1$), revealing the nonexponential character. Long persistence lengths and log-periodic oscillations prevent convergence towards Gaussian propagators, even if weak autocorrelation gives $H = 1/2$. Figures 3(c) and 3(d) present stronger and convincing evidence about the non-Gaussian behavior of the propagator within the region $0 < \delta < 1/2$. In Fig. 3(c) the difference $\Delta_3 = \langle (x - \langle x \rangle)^3 \rangle = 3\langle x \rangle [\langle x^2 \rangle - \langle x \rangle^2] - [\langle x^3 \rangle - \langle x \rangle^3]$ is shown as a function of $\ln t$. This difference must be equal to zero for a Gaussian distribution. We see that Δ_3 oscillates with ever growing amplitudes in a log-periodic fashion, which is supported by computing simulations. The errors involved in these experiments are no greater than 1%. From the log-log plot of Δ_3 for $\alpha > 0$ shown in the inset, we see that Δ_3 grows with time as a power law. The difference $\Delta_4 = 3[\langle x^2 \rangle^2 - \langle x \rangle^4] - [\langle x^4 \rangle - \langle x \rangle^4]$, which also must be identically zero for Gaussian distributions, is plotted in a log-log plot in Fig. 3(d). These results are evidence of the non-Gaussian character of the propagator. The inset shows the distribution of the position of the walker. Notice that the resemblance to a Gaussian distribution is misleading, in view of the discussions above. The plots in Figs. 3(c) and 3(d) were obtained for 50 000 time units with 20×10^6 runs.

In conclusion we have shown that the long-range memory effects lead to a change in the nature of the propagator of a normal diffusive regime. The departure from the expected Gaussian statistics breaks down the usual connection between the observed macroscopic behavior and the underlying microscopic statistics that ultimately govern the actions of the walker.

Acknowledgments. We thank FAPESP (Grants No. 2011/13685-6 and No. 2011/06757-0) and CNPq for funding.

[1] R. Metzler and J. Klafter, Phys. Rep. **339**, 1 (2000).
[2] R. Metzler and J. Klafter, J. Phys. A **37**, R161 (2004).
[3] G. Radons, R. Klages, and I. M. Sokolov, *Anomalous Transport* (Wiley-VCH, Berlin, 2008).
[4] M. F. Shlesinger, G. M. Zaslavsky, and J. Klafter, Nature (London) **363**, 31 (1993); *Lévy Flights and Related Topics in Physics*, edited by M. F. Shlesinger, G. Zaslavsky, and U. Frisch (Springer, Berlin, 1995).
[5] M. Kollmann, Phys. Rev. Lett. **90**, 180602 (2003).
[6] B. Lin, M. Meron, B. Cui, S. A. Rice, and H. Diamant, Phys. Rev. Lett. **94**, 216001 (2005).
[7] R. N. Mantegna and H. E. Stanley, *An Introduction to Econophysics* (Cambridge University Press, Cambridge, 2000).
[8] A. Weron and M. Magdziarz, Europhys. Lett. **86**, 60010 (2009).
[9] M. Magdziarz, A. Weron, K. Burnecki, and J. Klafter, Phys. Rev. Lett. **103**, 180602 (2009).
[10] K. Weron, A. Jurlewicz, M. Magdziarz, A. Weron, and J. Trzmiel, Phys. Rev. E **81**, 041123 (2010).
[11] M. Magdziarz and A. Weron, Phys. Rev. E **84**, 051138 (2011).
[12] K. Bumecki, J. Klafter, M. Magdziarz, and A. Weron, Phys. A **387**, 1077 (2008).
[13] K. Burnecki, J. Gajda, and G. Sikora, Phys. A **390**, 3136 (2011).
[14] B. Dybiec and E. Gudowska-Nowak, Chaos **20**, 043129 (2009).
[15] E. Gudowska-Nowak, B. Dybiec, P. F. Gora, and R. Zygadło, Acta Phys. Pol. B **40**, 1263 (2009).
[16] A. A. Stanislavsky, K. Burnecki, M. Magdziarz, A. Weron, and K. Weron, ApJ **693**, 1877 (2009).
[17] I. Eliazar and J. Klafter, J. Phys. A **43**, 132002 (2010).
[18] I. Eliazar and J. Klafter, Ann. Phys. (NY) **326**, 2517 (2011).
[19] C. W. Granger and R. Joyeux, J. Time Ser. Anal. **1**, 15 (1980).
[20] S. Q. Ling and W. K. Li, J. Am. Stat. Assoc. **92**, 1184 (1997).
[21] J. Beran, *Statistics for Long Memory Processes* (Chapman and Hall, New York, 1994).
[22] G. M. Schütz and S. Trimper, Phys. Rev. E **70**, 045101 (2004).
[23] J. C. Cressoni, M. A. A. da Silva, and G. M. Viswanathan, Phys. Rev. Lett. **98**, 070603 (2007).
[24] A. S. Ferreira, J. C. Cressoni, G. M. Viswanathan, and M. A. A. da Silva, Phys. Rev. E **81**, 011125 (2010).
[25] J. Klafter and I. M. Sokolov, Phys. World **18**(8), 29 (2005).
[26] NIST/SEMATECH e-Handbook of Statistical Methods, http://www.itl.nist.gov/div898/handbook/eda/section3/normprpl.htm.